Dynamics of biped robots during a complete gait cycle: Euler-Lagrange vs. Newton-Euler formulations

Hayder F N Al-Shuka, Burkhard Corves, Wen-Hong Zhu

Dynamics of biped robots during a complete gait cycle:
Euler-Lagrange vs. Newton-Euler formulations

Hayder F. N. Al-Shuka[1], Burkhard Corves[2], Wen-Hong Zhu[3]

1 School of Control Science and Engineering, Shandong University, Jinan, China

2 Department of Mechanism Theory, Machines Dynamics and Robotics, RWTH Aachen University, Germany

3 Canadian Space Agency, Canada

Abstract

The aim of this report is to derive the equations of motion for biped robot during different walking phases using two well-known formulations: Euler-Lagrange (E-L) and Newton-Euler (N-E) equations. The modeling problems of biped robots lie in their varying configurations during locomotion. They could be fully actuated during the single support phase (SSP) and overactuated during the double support phase (DSP). Therefore, first, the E-L equations of 6-link biped robot are described in some details for dynamic modeling during different walking phases with concentration on the DSP. Second, the detailed description of modified recursive Newton-Euler (N-E) formulation (which is very useful for modeling complex robotic system) is illustrated with a novel strategy for solution of the over-actuation/discontinuity problem. The derived equations of motion of the target biped for both formulations are suitable for control laws if the analyzer needs to deal with control problems. As expected, the N-E formulation is superior to the E-L concerning dealing with high degrees-of freedom (DOFs) robotic systems (larger than six DOFs).

Contents

1 Dynamic modeling

Humans have perfect mobility with amazing control systems; they are extremely versatile with smooth locomotion. However, comprehensive understanding of the human locomotion is entirely still not analyzed. Please see [Hay19, Hay18/1, Hay18/2, Hay18/3, Hay18/4, Hay17/1, Hay17/2, Hay16, Hay15, Hay14, Hay14/1, Hay14/2, Hay14/3, Hay14/4, Hay13/1, Hay13/2, Hay13/3, Sam08] for more details on dynamics, walking pattern generators and control of biped locomotion (biped robots, lower-extremity exoskeletons, prosthetics, etc.). To dynamically model the ZMP-based biped mechanisms, the following points should be considered:

- Biped robots are kinematically varying mechanisms such that they could be fully actuated during the SSP and over-actuated during the DSP. If we assume the biped robot as fixed-base mechanism, the dynamic modeling and control strategies of fixed-base manipulators can efficiently be used.
- Dealing with unilateral contact of the foot-ground interaction as a passive joint (rigid-to-rigid contact) or as compliant model (penalty-based approach).
- Reducing the number of links/joints of the target biped as possible. However, they can still have more than six DOFs resulting in computational problems of advanced control systems.
- Reducing the walking phases as much as possible, e.g., most conventional ZMP-based biped robots (see **Tab. 2.2** of [Hay14]) can walk with two substantial walking phases: the SSP and the DSP. Adjustments of the walking patterns are possible by modification of foot design as described in [Sat10].
- Most ZMP-based biped robots walks with flat swing /stance feet all the time; this can facilitate the analysis of biped locomotion by reducing walking phases to exactly two phases: the SSP and the DSP (see ref. [Van08]). However, heel-off/toe-off sub-phases can offer better characteristics but with careful analysis as we will see later.

In the light of the above comments, classical Euler-Lagrange (E-L) equations and recursive Newton-Euler (N-E) can be used for dynamic modeling of biped robots. For complex robotic systems, such as humanoid robots or any robot having the number of degrees of freedom (DOFs) larger than 6 DOFs, difficulties are encountered in the implementation of the control algorithms. Therefore, over 30 years, the robotics researchers have focused on the problem of computational efficiency. Many efficient O (n) algorithms have been developed for inverse [Sah99] and forward dynamics [Moh07] of robotic systems. For more literature on the efficient dynamic algorithms, refer to refs. [Kha11]. The adaptive control algorithm, however, which deals with controlling the robotic systems despite their uncertain parameters may decrease the computational efficiency of

the dynamics O (n) algorithms. Fu *et al.* [Fu87] have shown that the combined identification and control algorithms can be computed in O (n^3) time despite using the recursive (N-E) formulation. One of the efficient tools to deal with full-dynamics-based control for complex robotic systems is the virtual decomposition control (VDC) suggested by Zhu [Zhu10]. It is equivalent to the recursive NE formulation if the dynamic parameters of the target robotic system are known.

This work deals with the ZMP-based biped robot as a fixed-base robot with rigid foot-ground interaction. In addition, E-L equations are described in some details for dynamic modeling of the biped during different walking phases; problems of over-actuation/ discontinuity are resolved. Then detailed description of the VDC is illustrated with a novel strategy for solution of the over-actuation/discontinuity problem. The remainder of this report is organized as follows. Selection of the walking patterns suggested throughout the current work is presented in Section 1.1. Section 1.2 deals with detailed modeling of biped robot using the E-L equations and VDC. Section 2 concludes.

1.1 Selection of walking patterns

As mentioned earlier, different walking patterns can be constructed according to point view of the designer. In general, two walking patterns will be investigated throughout the current work; therefore, this report is interested with dynamic modeling of these walking patterns. The details of the DOFs for the referred walking patterns are as follows.

(i) According to **Fig. 1-1 (a)**, the walking pattern 1 has six generalized coordinates without constraints; the biped behaves as an open-chain mechanism. Consequently, the biped has six DOFs in this walking phase with six links (neglecting the stance-foot link). Whereas, it has seven generalized coordinates with seven links during the DSP due to the rotation of the front foot, but with two constraints equations; the tips of the front and rear feet are fixed(see **Fig. 1-1**). Consequently, the biped has five DOFs during this constrained walking phase, DSP, with six actuators (over-actuated system).

(ii) The walking pattern 2 has also six DOFs with six links during the SSP; it has the same configuration of walking pattern 2. The first sub-phase of DSP (henceforth called DSP1) has six generalized coordinates with two constraint equations; therefore, the biped has 4 DOFs with 6 actuators (over-actuated system). During the second sub-phase of DSP (henceforth called DSP2), similar configurations of that of DSP1 appear and consequently the biped has four DOFs and six actuators. Both DSP1 and DSP2 have six links as shown in **Fig. 1-2 (a)** and **(b)** respectively.
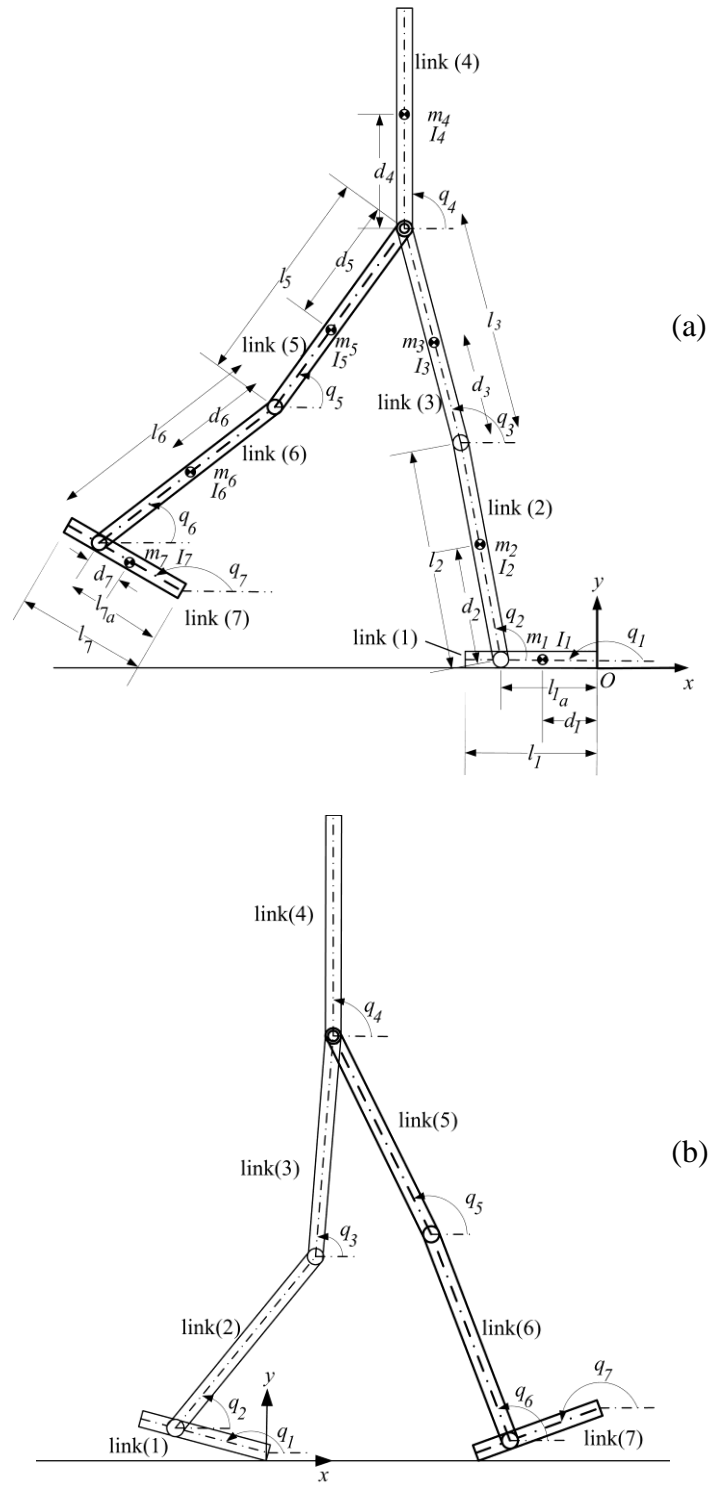
Fig. 1-1: Walking pattern 1 with description of generalized coordinates. (a) Intermediate configuration of biped locomotion during the SSP. (b) Intermediate configuration of biped locomotion during the DSP.
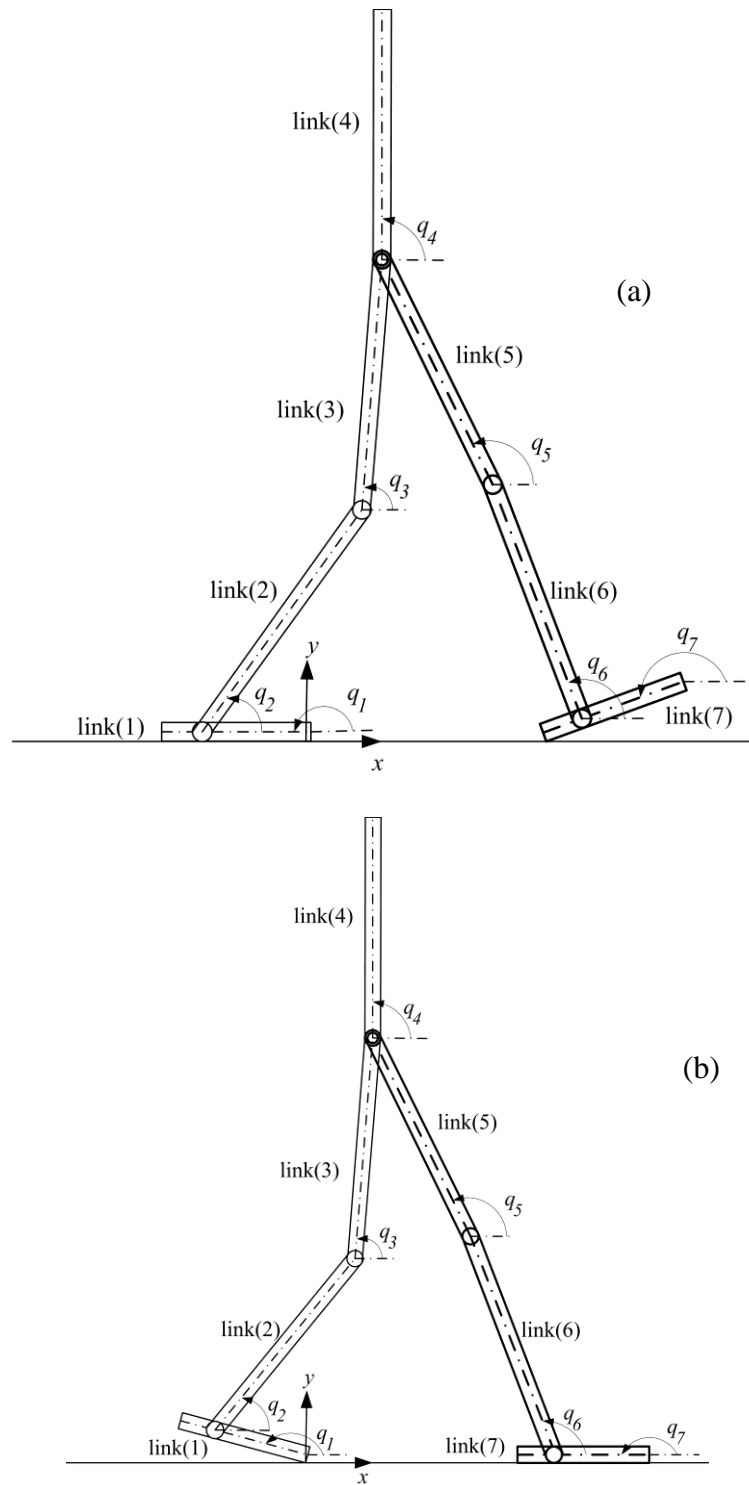
Fig. 1-2: Walking pattern 2 with description of generalized coordinates. (a) Intermediate configuration of biped locomotion during the DSP1; link (1) has negligible dynamics in such case. (b) Intermediate configuration of the biped locomotion during the DSP2; link (7) has negligible dynamics in such case.

1.2   Dynamic modeling

As mentioned previously, two approaches are commonly used to obtain the differential equations of motions: E-L and N-E formulations. Depending on the purpose of the analyzer/designer, various forms of modified formulations have been conducted such as recursive E-L equations [Hol80], recursive N-E formulation [Moh07], and generalized D'Alembert (G-D) formulation [Lee83]. This work concentrates on formulating the dynamic equations that are suitable for adaptive control purposes. Throughout the current analysis, the following assumptions have been proposed.

Assumption 1-1. The stance foot, link (1), is in full contact with the ground during the SSP; therefore, its dynamics could be neglected in such case.

Assumption 1-2. The foot-ground contact is rigid-to-rigid contact. Accordingly, the tips of the feet (in case of foot rotation) are assumed passive joints.

Assumption 1-3.There are only two substantial walking phases, the SSP and the DSP, with possibly sub-phases during the DSP. The instantaneous impact event is avoided by making the swing foot contact the ground with zero velocity (disadvantage of zero end velocity at impact is the higher energy consumption due to need for braking in swing leg).

In biped systems, three important aspects should be taken into consideration:

(i)   Preventing the biped legs from slippage.
(ii) Avoiding discontinuities of the ground reaction forces which can result in discontinuities of the actuator torques as detailed in Section 1.2.1.3
(iii) Concentrating on the adaptive control of the biped robot associated with less computational complexity.

1.2.1   The Euler-Lagrange formulation

Although the E-L equations can provide closed-form state equations suitable to advanced control strategies, their computational complexity, unless it is simplified, could be inefficient for analysis/control of complex robotic system (more than 6 DOFs) [Zhu10]. In fact, E-L formulation could be used recursively [Hol80]; it has been equivalent to recursive N-E formulation in most all aspects [Spo89]. In general, the computational complexity of E-L, N-E and G-D are $O(n^4) or O(n^3), O(n)$ and $O(n^3)$ respectively. Below we present modeling of biped robot during the two phases: the SSP and the DSP with two different kinds of Lagrange equations.

1.2.1.1 E-L equations of the second kind (the SSP)

The E-L equations for open chain mechanism (biped robot during the SSP) can be expressed as

$$\frac{d}{dt}\left(\frac{\partial L}{\partial \dot{q}_i}\right) - \frac{\partial L}{\partial q_i} = T_i \quad (i = 1, 2, \ldots \ldots, n_q)$$

Eq. 1-1

where L is Lagrangian function which is equal to the kinetic energy of the robotic system (K) minus its potential energy (P), q_i denotes the generalized coordinates of link (i), and $\dot{q}_i$ is the derivative of the generalized coordinates.

The generalized coordinates are a set of coordinates that completely describes the location (configuration) of the dynamic systems relative to some reference configuration [Fu87]. There are many choices to select these generalized coordinates; however, the joint/link displacements are proved being suitable in case of robotic systems. If the number of these generalized coordinates is equal to the degrees of freedom of the target system, then **Eq. 1-1** is valid; **Eq. 1-1** is called Lagrange equations of the second kind and it suitable for open-chain mechanism. Solution of **Eq. 1-1** can result in the following second order differential equations.

$$\boldsymbol{M}(\boldsymbol{q})\ddot{\boldsymbol{q}} + \boldsymbol{C}(\boldsymbol{q}, \dot{\boldsymbol{q}})\dot{\boldsymbol{q}} + \boldsymbol{g}(\boldsymbol{q}) = \boldsymbol{A}(\boldsymbol{\tau} - \boldsymbol{\tau}_f)$$

or simply,

$$\boldsymbol{M}(\boldsymbol{q})\ddot{\boldsymbol{q}} + \boldsymbol{C}(\boldsymbol{q}, \dot{\boldsymbol{q}})\dot{\boldsymbol{q}} + \boldsymbol{g}(\boldsymbol{q}) + \boldsymbol{A}\boldsymbol{\tau}_f = \boldsymbol{A}\boldsymbol{\tau}$$

Eq. 1-2

where $\boldsymbol{M} \in \mathbb{R}^{n_q \times n_q}$ is the mass matrix, $\boldsymbol{q}, \dot{\boldsymbol{q}}$ and $\ddot{\boldsymbol{q}} \in \mathbb{R}^{n_q}$ are the absolute angular displacement, velocity and acceleration of the robot links, $\boldsymbol{C} \in \mathbb{R}^{n_q \times n_q}$ represents the Coriolis and centripetal robot matrix, $\boldsymbol{g} \in \mathbb{R}^{n_q \times 1}$ is the gravity vector, $\boldsymbol{A} \in \mathbb{R}^{n_q \times n_\tau}$ is a mapping matrix derived by the principle of the virtual work, $\boldsymbol{\tau} \in \mathbb{R}^{n_\tau \times 1}$ is the actuating torque vector, n_τ represents the number of actuators, and $\boldsymbol{\tau}_f \in \mathbb{R}^{n_\tau \times 1}$ represents the dissipative torques resulted from joint friction.

In the following, some details are presented to determine the dynamic coefficient matrices of **Eq. 1-2**.

   (i) Inertia matrix

The derivation, structure and properties of the mass matrix ($\boldsymbol{M}$) can be obtained from the total kinetic energy of the biped system. The velocity wrench, $\bar{\boldsymbol{v}}_i \in \mathbb{R}^{6 \times 1}$, of link ($i$) can be expressed in term of Jacobian matrices as follows [Spo89, Fu87].

$$\overline{v}_i = \begin{bmatrix} v_i \\ w_i \end{bmatrix} = \begin{bmatrix} J_{vi} \\ J_{wi} \end{bmatrix} \dot{q} \qquad \text{Eq. 1-3}$$

with $v_i \in \mathbb{R}^{3 \times 1}$ and $w_i \in \mathbb{R}^{3 \times 1}$ are the translational and angular velocity components of link (i), $J_{vi} \in \mathbb{R}^{3 \times n_q}$ and $J_{wi} \in \mathbb{R}^{3 \times n_q}$ denote the Jacobian matrices associated with translation and rotation components respectively.

The total kinetic energy of $n - $ DOF robotic system can be expressed as

$$K = \sum_{i=1}^{n} K_{vi} + \sum_{i=1}^{n} K_{wi} = \frac{1}{2}\sum_{i=1}^{n} \dot{q}^T (J_{vi}^T \, m_i \, J_{vi})\dot{q} + \frac{1}{2}\sum_{i=1}^{n} \dot{q}^T (J_{wi}^T \, \mathfrak{I}_i J_{wi})\dot{q} = \frac{1}{2}\dot{q}^T \, M \, \dot{q} \qquad \text{Eq. 1-4}$$

where $\mathfrak{I}_i$ is the inertia tensor of link (i) relative to the inertial coordinate frame; it is a configuration-dependent parameter. Using similarity transformation [Spo89], it is necessary to express the inertia tensor in terms of body frame to get the configuration-free inertia tensor, I_i, as follows

$$\mathfrak{I}_i = R(q)I_i R^T(q) \qquad \text{Eq. 1-5}$$

Thus, the mass matrix of the biped mechanism can be defined as

$$M = \sum_{i=1}^{n} J_{vi}^T \, m_i \, J_{vi} + \sum_{i=1}^{n} J_{wi}^T \, R(q) \, I_i R^T(q) J_{wi} \qquad \text{Eq. 1-6}$$

(ii) Coriolis and centripetal terms

Following the detailed derivation of [Spo89, Fu87], without showing the details here, the $(k,j)^{th}$ element of the Coriolis and centripetal matrix can be defined as

$$c_{kj} = \frac{1}{2}\sum_{i=1}^{n} \left[\frac{\partial m_{kj}}{\partial q_i} + \frac{\partial m_{ki}}{\partial q_j} - \frac{\partial m_{ij}}{\partial q_k} \right] \dot{q}_i \qquad (k, j = 1,2, \dots, n) \qquad \text{Eq. 1-7}$$

with m_{ij} denotes an element of mass matrix with row index, i, and column index, j.

(iii) Gravity term

This term can be derived from the total potential energy of the biped system as follows.

$$P = \sum_{i=1}^{n} m_i \boldsymbol{g}_i^T \boldsymbol{c}_i \qquad\qquad\qquad \textbf{Eq. 1-8}$$

where $\boldsymbol{g}_i$ denotes the gravitational acceleration vector of link (i); for plane system it is equal to $[0 \quad -9.81 \quad 0]^T$. Every element of the gravitational term of **Eq. 1-2** can be expressed as

$$g_k = -\frac{\partial P}{\partial \boldsymbol{q}_k} \qquad (k = 1,2, \dots \dots, n) \qquad\qquad \textbf{Eq. 1-9}$$

   (iv) The mapping matrix A

This mapping (coordinates transformation) matrix can be determined by the principle of the virtual work. The virtual work, W, of the generalized link torques acting on the biped system can be expressed in terms of generalized link coordinates as

$$\delta W = T_1 \delta q_1 + T_2 \delta q_2 + \cdots + T_{n_q} \delta q_{n_q} \qquad\qquad \textbf{Eq. 1-10}$$

with T_i denote the generalized torque of link (i) associated with its generalized coordinate, q_i.

Eq. 1-10 can be re-written in a vector form as

$$\delta W = \boldsymbol{T}^T \, \delta \boldsymbol{q} \qquad\qquad\qquad \textbf{Eq. 1-11}$$

Let $\boldsymbol{\theta} \in \mathbb{R}^{n_q}$ be the generalized joint coordinates; thus, we can get a linear relationship between links and joint coordinates as follows.

$$\delta \boldsymbol{q} = \boldsymbol{A}^{-T} \, \delta \boldsymbol{\theta} \qquad\qquad\qquad \textbf{Eq. 1-12}$$

Substituting **Eq. 1-12** into **Eq. 1-11**, we have

$$\delta W = \boldsymbol{T}^T \boldsymbol{A}^{-T} \, \delta \boldsymbol{\theta} \qquad\qquad\qquad \textbf{Eq. 1-13}$$

$$\boldsymbol{T} = \boldsymbol{A}\boldsymbol{\tau} \qquad\qquad\qquad \textbf{Eq. 1-14}$$

Remark 1-1. Alternatively, the matrix $\boldsymbol{A}$ can be found simply according to the principle of free-body diagram as done in [Van08].

   (v) Friction torques and other disturbance sources

In effect, the friction terms are complex and may be modeled approximately using the following form [Zhu10]

$$\tau_{f_i} = coulomb\ friction + viscous\ friction + Stribeck\ friction$$
$$+ friction\ offset\ term$$

Eq. 1-15

$$= \hbar_{ci}\ sign(\dot{\theta}_i) + \hbar_{vi}\dot{\theta}_i + \hbar_{si}\ sign(\dot{\theta}_i) \exp\left(-\left(\dot{\theta}_i/\eta_{si}\right)\right) + \hbar_{oi} \quad (i = 1,2,\dots n)$$

where $\dot{\theta}_i$ represents the angular joint velocity of each link, $\hbar_{ci}$, $\hbar_{vi}$ and $\hbar_{si}$ denote the Coulomb friction coefficient, viscous friction coefficient, and Stribeck friction effect respectively, and $\hbar_{oi}$ is the friction offset term.

As we see from **Eq. 1-15**, friction has a local effect; the vector of friction torque is uncoupled.

In the light of the above formulae, **Eq. 1-2** can be re-written as

$$\sum_{j=1}^{n} m_{kj}(q)\ddot{q}_j + \sum_{j=1}^{n} c_{kj}(q)\ \dot{q}_j + g_k(q) + T_{fk} = T_k \quad (k = 1,2,\dots,n)$$

Eq. 1-16

with T_{fk} represents the friction torque affecting each link.

Remark 1-2. There are several fundamental properties of the dynamic coefficient matrices, the mass matrix and the Coriolis and centripetal terms, which could be exploited in controller design of adaptive control. For more details on other properties, refer to [Spo89].

Property 1-1. The mass matrix (M) is symmetric and positive definite. This can be deduced from **Eq. 1-4** and the property of the kinetic energy.

Property 1-2. The matrix $\dot{M}(q) - 2C(q,\dot{q})$ is skew matrix, if the $C(q,\dot{q})$ matrix is described in terms of Christoffel symbols, **Eq. 1-7**. Proof of this property can be found in [Spo89].

Property 1-3. The dynamic equations described in **Eq. 1-2** are dependent linearly on certain parameters such as link masses, moment of inertia, friction coefficients etc.; consequently

$$M(q)\ddot{q} + C(q,\dot{q})\dot{q} + g(q) + A\tau_f = Y(q,\dot{q},\ddot{q})\alpha$$

Eq. 1-17

where $Y(q,\dot{q},\ddot{q}) \in \mathbb{R}^{n \times n_\alpha}$ is called the regressor matrix, a function of the known generalized coordinates and their first two derivatives, and $\alpha \in \mathbb{R}^{n_\alpha}$ denotes the vector of unknown biped parameters.

Selection of α is not unique, and it is difficult to find minimal set of these parameters [Spo89]. **Eq. 1-17** is very important to adaptive control.

1.2.1.2 The E-L equations of the first kind (the DSP)

As mentioned earlier, the biped mechanism constitutes a closed-chain with over-actuation during the DSP. Therefore, the Lagrange formulation of the 1st kind, which can deals with constraints, is needed for dynamic modeling of the constrained biped. In such case, the motion equations are represented by redundant coordinates resulting in differential algebraic equations DAEs. The algebraic equations result from the constraints derived from the kinematics [Tsa99]. The constraints can be easily incorporated into the main equations using Lagrange multipliers. The Lagrange equations of the biped robot during the DSP can be defined as

$$\frac{d}{dt}\left(\frac{\partial L}{\partial \dot{q}_i}\right) - \frac{\partial L}{\partial q_i} = T_i + \sum_{j=1}^{n_c} \lambda_j \frac{\partial \varphi_j}{\partial q_i} \qquad (i = 1, 2, \ldots \ldots, n_q)$$

Eq. 1-18

where φ_j denotes the constraint function of each closed loop, n_c is the number of these constraints, λ_j is the Lagrange multipliers associated with each constraint. Here n_q is the number of redundant generalized coordinates and equal to the number DOFs (n) of the biped systems plus the number of constraints(n_c).

Eq. 1-18 can be solved using two well-known techniques [Pen07]: the redundant coordinates-based techniques which are used mainly in commercial software such as MSC ADAMS, and the minimum coordinates-based techniques which could be, to some extent, suitable for control strategies and real-time applications. Many researchers have preferred the former technique due to its simplicity and ease of derivation at the expense of difficulties of numerical methods encountered in the solution [Pen07]. Consequently, this motivates the researchers to investigate the second technique which includes eliminating the constraint equations (Lagrange multipliers) from **Eq. 1-18** to result in constraint-free differential equations [Pen07]. This can be implemented using one of the orthogonalization methods which are [Pen07]: coordinate partitioning method, zero-eigenvalue method, singular value decomposition (SVD), QR decomposition, Udwadia-Kabala formulation, PUTD method, and Schur decomposition. For more details, see [Pen07].

Solution of **Eq. 1-18** results in

$$M(q)\ddot{q} + C(q,\dot{q})\dot{q} + g(q) + A\tau_f = A\tau + J^T\lambda$$

Eq. 1-19

$$\varphi(q) = 0$$

Eq. 1-20

with $\boldsymbol{\varphi} \in \mathbb{R}^{n_c}$ is the constraint vector, and $\boldsymbol{J} \in \mathbb{R}^{n_c \times n_q} = \frac{\partial \boldsymbol{\varphi}(q)}{\partial q}$ denotes the Jacobian matrix.

Remark 1-3. The coefficient dynamic matrices (mass matrix, Coriolis and centripetal matrix etc.) of **Eq. 1-19** could be determined by the same mathematical formulae defined in the open-chain mechanism as in **Eq. 1-6** to **Eq. 1-8**

To reduce the dimension size of **Eq. 1-19** (to eliminate $\boldsymbol{\lambda}$), a relationship between the redundant generalized coordinates ($\boldsymbol{q}$)and the independent coordinates ($\boldsymbol{q}_{in} \in \mathbb{R}^n$) should be found. In this report, the coordinate partitioning is used for size reduction of the equation of motion [Mit97].

Twice differentiating **Eq. 1-20** can result in

$$J(q)\dot{q} = 0 \qquad\qquad \textbf{Eq. 1-21}$$

$$J(q)\ddot{q} + \dot{J}(q, \dot{q})\dot{q} = 0 \qquad\qquad \textbf{Eq. 1-22}$$

Due to the redundancy of coordinates in **Eq. 1-19**, it is possible to express the dependent generalized coordinates in terms of the independent ones as in **Eq. 1-23**.

$$q_{in} = \breve{\varphi}(q)q \qquad\qquad \textbf{Eq. 1-23}$$

Twice differentiating **Eq. 1-23** yields

$$\dot{q}_{in} = J_r(q)\dot{q} \qquad\qquad \textbf{Eq. 1-24}$$

with $J_r(q) \in \mathbb{R}^{n \times n_q} = \frac{\partial \breve{\varphi}(q)}{\partial q}$

$$\ddot{q}_{in} = J_r(q)\ddot{q} + \dot{J}_r(q)\dot{q} \qquad\qquad \textbf{Eq. 1-25}$$

Blocking together **Eq. 1-21** and **Eq. 1-24** to get

$$\begin{bmatrix} J(q) \\ J_r(q) \end{bmatrix} \dot{q} = \begin{bmatrix} 0 \\ \dot{q}_{in} \end{bmatrix} \qquad\qquad \textbf{Eq. 1-26}$$

Thus, it is possible to get the following important relations

$$\dot{q} = \begin{bmatrix} J(q) \\ J_r(q) \end{bmatrix}^{-1} \begin{bmatrix} 0 \\ \dot{q}_{in} \end{bmatrix} = [\breve{F} \quad F] \begin{bmatrix} 0 \\ \dot{q}_{in} \end{bmatrix} = F(q)\dot{q}_{in} \qquad\qquad \textbf{Eq. 1-27}$$

The matrix $F \in \mathbb{R}^{n_q \times n}$ plays an important role in eliminating λ; the following orthogonality condition holds

$$J(q)F(q) = 0 \qquad \text{Eq. 1-28}$$

Differentiating **Eq. 1-27** to obtain

$$\ddot{q} = F(q)\,\ddot{q}_{in} + \dot{F}(q,\dot{q})\,\dot{q}_{in} \qquad \text{Eq. 1-29}$$

Substituting **Eq. 1-27** and **Eq. 1-29** into **Eq. 1-19** to get

$$M(q)\big(F(q)\ddot{q}_{in} + \dot{F}(q,\dot{q})\dot{q}_{in}\big) + C(q,\dot{q})F(q)\dot{q}_{in} + g(q) + A\tau_f = A\tau + J(q)^T\lambda \qquad \text{Eq. 1-30}$$

Alternatively, **Eq. 1-30** can be re-written as

$$\overline{M}(q)\ddot{q}_{in} + \overline{C}(q,\dot{q})\dot{q}_{in} + g(q) + A\tau_f = A\tau + J(q)^T\lambda \qquad \text{Eq. 1-31}$$

with

$$\overline{M}(q) = M(q)F(q),\ \overline{C}(q,\dot{q}) = M(q)\dot{F}(q,\dot{q}) + C(q,\dot{q})F(q) \qquad \text{Eq. 1-32}$$

Using **Eq. 1-27** and **Eq. 1-30** can yield

$$\lambda = \breve{F}(q)^T\big(\overline{M}(q)\ddot{q}_{in} + \overline{C}(q,\dot{q})\dot{q}_{in} + g(q) + A\tau_f - A\tau\big) \qquad \text{Eq. 1-33}$$

Exploiting **Eq. 1-28** and pre-multiplying **Eq. 1-31** by $F(q)^T$ to obtain

$$F(q)^T\overline{M}(q)\,\ddot{q}_{in} + F(q)^T\overline{C}(q,\dot{q})\dot{q}_{in} + F(q)^T g(q) + F(q)^T A\tau_f = F(q)^T A\tau \qquad \text{Eq. 1-34}$$

Remark 1-4. Although most researchers have written the matrices, $F(q)$, $\overline{M}(q)$, and $\overline{C}(q,\dot{q})$, in terms of the independent coordinates (q_{in}), these matrices still contain the dependent coordinates (q). Therefore, we have expressed the mentioned matrices in terms of the last coordinates.

Remark 1-5. The matrix $F(q)$ is not unique; the orthogonalization methods mentioned at the beginning of this subsection are used to get the matrix $F(q)$. Pennesri and Valentini [Pen07] simulated simple pendulum to compare the computational complexity of these orthogonalization methods. QR decomposition ranked best among the other methods. However, all these techniques could be computationally unsuitable to deal with the advanced adaptive control.

Remark 1-6. Eq. 1-31 has the same properties of that of **Eq. 1-2** as follows [Su90].

Property 1-4. Let $D(q) = F(q)^T \bar{M}(q), H(q, \dot{q}) = F(q)^T \bar{C}(q, \dot{q}),$ then the matrix $N(q, \dot{q}) = \dot{D}(q, \dot{q}) - 2H(q, \dot{q})$ is skew-matrix.

Proof. Let

$$N = \dot{D} - 2H \qquad \qquad \textbf{Eq. 1-35}$$

By substituting **Eq. 1-32** into **Eq. 1-35** we get

$$N = \dot{F}^T M F + F^T \dot{M} F + F^T M \dot{F} - 2F^T M \dot{F} - F^T C F$$

$$= F^T (\dot{M} - 2C)F + \dot{F}^T M F - F^T M \dot{F} = F^T (\dot{M} - 2C)F \qquad \qquad \textbf{Eq. 1-36}$$

Since $\dot{M} - 2C$ is skew-matrix according to Property 1-1, then N is also skew-matrix.

Property 1-5. The orthogonality condition is satisfied by the matrix $F(q)$ such that **Eq. 1-28** holds.

Proof. From **Eq. 1-21** and substituting **Eq. 1-27,** we have

$$JF\,\dot{q}_{in} = 0 \qquad \qquad \textbf{Eq. 1-37}$$

Since $\dot{q}_{in}$ is linearly independent, then

$$JF = F^T J^T = 0 \qquad \qquad \textbf{Eq. 1-38}$$

Property 1-6. If $F(q)$ is known, then the left hand side of **Eq. 1-31** are linearly dependent on the unknown biped parameters (the same Property 1-3).

1.2.1.3   Continuous dynamic response

One of the inherent problems of legged locomotion (bipeds, quadrupeds, etc.) is the discontinuity at the transition instances due to: (i) impact events; these can be avoided by setting the foot velocity equal to zero at the instance of contact (see Chapters 5 and 6 of [Hay14]), and (ii) varying configurations of the biped from the SSP to the DSP and vice versa. As said previously in Section 1.1, the number of actuators is more than the DOFs of the biped during the constrained DSP. This means that there are infinity combinations of actuator torques to drive the biped systems as explained below.

One of the methods for determining the actuating torques and the ground reaction forces is the pseudo-inverse matrix as follows.

Eq. 1-19 can be re-arranged to yield

$$M(q)\ddot{q} + C(q,\dot{q})\dot{q} + g(q) + A\tau_f = [A \quad J(q)^T]\begin{bmatrix}\tau\\\lambda\end{bmatrix}$$

Eq. 1-39

One of the possible solutions to get the actuating torques and Lagrange multipliers are

$$\begin{bmatrix}\tau\\\lambda\end{bmatrix} = [A \quad J^T]^{\neq}(M(q)\ddot{q} + C(q,\dot{q})\dot{q} + g(q) + A\tau_f)$$

Eq. 1-40

where the notation $[.]^{\neq}$ denotes the pseudo-inverse of the referred matrix.

As seen from **Eq. 1-40**, there is no guarantee that τ and λ have the same values at the start/end of the SSP due to this optimization solution. Therefore, the following assumption is proposed to resolve this dilemma.

Assumption 1-4. Because the biped robot does not have a unique solution during the DSP, a linear transition function could be proposed for the ground reaction forces [Alb12]. Thus, for the front foot

$$\lambda = \left(\frac{t - t_s}{t_d - t_s}\right) m_G(\ddot{c}_G + [0, g, 0]^T)$$

Eq. 1-41

where t, t_s and t_d are time parameter, the time of SSP, and the DSP time. Meanwhile, the ground reaction forces, $\bar{\lambda}$, of the rear foot are

$$\bar{\lambda} = m_G(\ddot{c}_G + [0, g, 0]^T) - \lambda$$

Eq. 1-42

Accordingly, at the initial instance of DSP, $\lambda = 0$, and the full ground reaction forces are supported by the rear foot, whereas, at the end of the DSP, the full support appears to be in the front foot with $\bar{\lambda} = 0$. On the other hand, because COG acceleration of the biped is nonlinear, the resulted ground reaction forces from **Eq. 1-41** can generate nonlinear profile despite of multiplication of the latter equation with linear scaling function.

1.2.2   The modified recursive N-E formulation

Due to computational complexity inherent in the classical Lagrangian formulation, unless it is simplified, the researchers have resorted to the recursive N-E formulation for real time implementation. The philosophy of deriving N-E formulation is different from that of Lagrangian formulation. In the former, the translation/angular equations of motion of each link are derived sequentially using the D'Alembert principle. Due to the coupling effect between each neighbored

links and appearance the translation equations of motion, the coupling force wrench appears in the derivation. Then a set of forward and backward recursive equations is used to determine the velocity and force wrenches respectively [Spo89, Fu87]. Various forms of N-E formulations for different robotic mechanism have been investigated; for details refer to [Kha11].

However, Fu *et al.* [Fu87] have shown that the combined identification and control algorithms can be computed in $O(n^3)$ despite using recursive N-E formulation. Strictly speaking, dealing with advanced adaptive control techniques, the recursive N-E formulations could not be powerful; a modification is needed to satisfy the desired target. Zhu [Zhu10] exploited the recursive nature of N-E equations to virtually decompose complex robotic systems into subsystems and to use the advanced adaptive techniques recursively. The derivation is exactly of that of recursive N-E formulation, but the difference is that the VDC derives the equation of motion of each link in terms of a frame attached at it first end rather than its COM.

1.2.2.1   Derivation of the dynamic equations

Now let us consider a fixed base serial-chain manipulator with revolute and prismatic joints. Thus, the links are numbered from 1 to n_q, where the base link is numbered as zero link. **Fig. 1-3** shows link (i) where $i = 1,2, \ldots., n_q,$ is connected to other links via mechanical joints at its ends. This link has one driving cutting point associated with the frame $\{T_{i+1}\}$ and one driven cutting point associated with the frame $\{B_i\}$. Thus, the joint (i) has one driven cutting point associated with the frame $\{B_i\}$ and one driving cutting point associated with the frame $\{T_i\}$.

Below, we will illustrate some remarks to make the derivation of dynamic equation of each subsystem (link, joint) accessible.
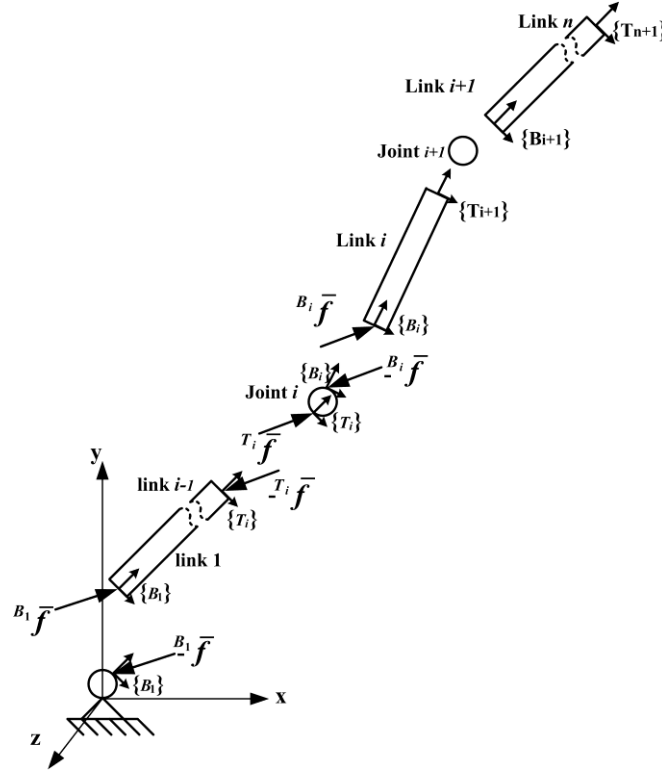
Fig. 1-3: Virtual decomposition of a serial-chain manipulator

Remark 1-7. [Zhu10]. The matrix of force wrench transformation, ${}^{B}U_{A} \in \mathbb{R}^{6\times6}$, transforms the force wrench expressed in frame $\{A\}$ to the same force wrench expressed in frame $\{B\}$ as follows.

$$ {}^{B}\bar{f} = {}^{B}U_{A} \, {}^{A}\bar{f} \qquad\qquad \textbf{Eq. 1-43} $$

with

$$ {}^{B}U_{A} = \begin{bmatrix} {}^{B}R_{A} & 0_{3\times3} \\ ({}^{B}r_{BA} \times)\,{}^{B}R_{A} & {}^{B}R_{A} \end{bmatrix} \qquad\qquad \textbf{Eq. 1-44} $$

where ${}^{B}R_{A} \in \mathbb{R}^{3\times3}$ refers to the rotation matrix from the frame $\{A\}$ to the frame $\{B\}$, $0_{3\times3}$ is 3×3 null matrix, $({}^{B}r_{BA} \times)$ is the skew matrix of the vector ${}^{B}r_{BA}$, which represents a vector from the origin of frame $\{B\}$ to the origin of frame $\{A\}$, expressed by

$$ ({}^{B}r_{BA} \times) = \begin{bmatrix} 0 & -{}^{B}r_{BA)z} & {}^{B}r_{BA)y} \\ {}^{B}r_{BA)z} & 0 & -{}^{B}r_{BA)x} \\ -{}^{B}r_{BA)y} & {}^{B}r_{BA)x} & 0 \end{bmatrix} \qquad\qquad \textbf{Eq. 1-45} $$

whereas the transpose of ${}^{B}U_{A}$ can transform the velocity wrench from frame to another as follows.

$$
{}^{A}\overline{v} = {}^{B}U_{A}^{T} \ {}^{B}\overline{v} \qquad\qquad \textbf{Eq. 1-46}
$$

Remark 1-8. The net force wrench of link (i) can be sequentially expressed in terms of frame $\{B_i\}$ as

$$
{}^{B_i}\overline{f}^{*} = {}^{B_i}\overline{f} - {}^{B_i}U_{T_{i+1}} \ {}^{T_{i+1}}\overline{f} \qquad\qquad \textbf{Eq. 1-47}
$$

Exploiting Remark 1-7 to yield

$$
{}^{B_i}\overline{f}^{*} = {}^{B_i}\overline{f} - {}^{B_i}U_{T_{i+1}} \ {}^{T_{i+1}}U_{B_{i+1}} \ {}^{B_{i+1}}\overline{f} = {}^{B_i}\overline{f} - {}^{B_i}U_{B_{i+1}} \ {}^{B_{i+1}}\overline{f} \qquad\qquad \textbf{Eq. 1-48}
$$

Remark 1-9. The velocity wrench of link (i) can sequentially be determined by

$$
{}^{B_i}\overline{v} = z \ \dot{q}_i + {}^{B_{i-1}}U_{B_i}^{T} \ {}^{B_{i-1}}\overline{v} \qquad\qquad \textbf{Eq. 1-49}
$$

with $z = [0\ 0\ 0\ 0\ 0\ 1]$ or $[0\ 0\ 1\ 0\ 0\ 0]$ for revolute and prismatic joints respectively. Alternatively and simply, the velocity wrench can be calculated as

$$
{}^{B_i}\overline{v} = \begin{bmatrix} {}^{B_i}R_I v_{B_i} \\ {}^{B_i}R_I w_{B_i} \end{bmatrix} \qquad\qquad \textbf{Eq. 1-50}
$$

with $v_{B_i} \in \mathbb{R}^3$ and $w_{B_i} \in \mathbb{R}^3$ are the absolute translational and angular velocity vector of frame B_i respect to the inertial frame $\{I\}$.

Remark 1-10. Concerning the target biped, the number of the generalized coordinates (n_q) is always equal to the number of links, e.g. both the number of links and the generalized coordinates are equal to six during the SSP. Consequently, we named the number of links as that of generalized coordinates.

(i) Dynamics of link subsystem

By applying the D'Alembert principle to link (i), with respect to the inertial frame about the COM of link (i), we can get the following relations for the net forces $\overline{f}_i^{*}$ and the net moment $\overline{m}_i^{*}$, as shown in **Fig. 1-4**.
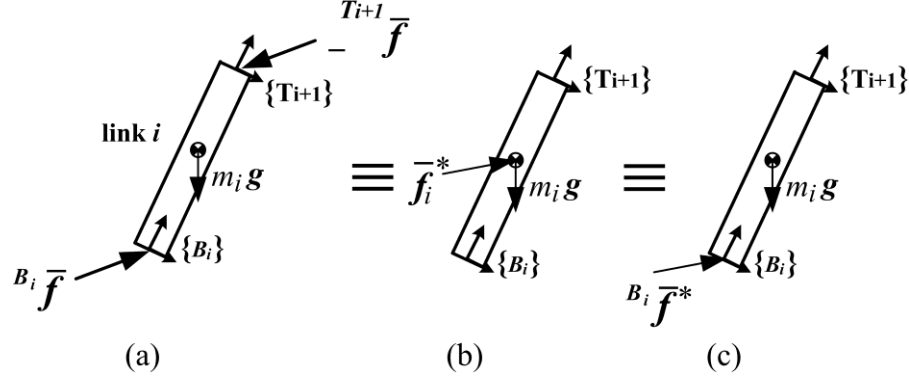
Fig. 1-4: Virtual decomposition of link (i) with description of the net force wrench. (a) The free-body diagram of the link (i) with force wrench at its ends and gravity effect. (b) The net force wrench applied at the COG of link (i) with gravity effect. (c) The net force wrench applied at one end of link (i) with gravity effect.

$$f_i^* = \frac{d(m_i\, \boldsymbol{v}_i)}{dt} = m_i\, \dot{\boldsymbol{v}}_i + m_i\, \boldsymbol{g} \qquad\qquad \textbf{Eq. 1-51}$$

$$\boldsymbol{m}_i^* = \frac{d(I_i(t)\widehat{\boldsymbol{w}}_i)}{dt} = \mathcal{I}_i(t)\, \dot{\boldsymbol{w}}_i + (\boldsymbol{w}_i \times)\mathcal{I}_i(t)\boldsymbol{w}_i = \mathcal{I}_i(t)\, \dot{\boldsymbol{w}}_i + \boldsymbol{w}_i \times (\mathcal{I}_i(t)\boldsymbol{w}_i) \qquad \textbf{Eq. 1-52}$$

where $\boldsymbol{v}_i \in \mathbb{R}^{3\times 1}$ refers to the translation velocity vector of each link.

Putting **Eq. 1-51** and **Eq. 1-52** into block matrix to deal with velocity and force wrenches

$$\begin{bmatrix} m_i\, \boldsymbol{I}_3 & \boldsymbol{0}_{3\times 3} \\ \boldsymbol{0}_{3\times 3} & \mathcal{I}_i(t) \end{bmatrix} \begin{bmatrix} \dot{\boldsymbol{v}}_i \\ \dot{\boldsymbol{w}}_i \end{bmatrix} + \begin{bmatrix} m_i\, \boldsymbol{g} \\ (\boldsymbol{w}_i \times)\mathcal{I}_i(t)\boldsymbol{w}_i \end{bmatrix} = \begin{bmatrix} f_i^* \\ \boldsymbol{m}_i^* \end{bmatrix} \qquad\qquad \textbf{Eq. 1-53}$$

or

$$\begin{bmatrix} m_i\, \boldsymbol{I}_3 & \boldsymbol{0}_{3\times 3} \\ \boldsymbol{0}_{3\times 3} & \mathcal{I}_i(t) \end{bmatrix} \dot{\bar{\boldsymbol{v}}}_i + \begin{bmatrix} m_i\, \boldsymbol{g} \\ (\boldsymbol{w}_i \times)\, \mathcal{I}_i(t)\boldsymbol{w}_i \end{bmatrix} = \bar{f}_i^* \qquad\qquad \textbf{Eq. 1-54}$$

with $\boldsymbol{I}_3$ is 3×3 identity matrix.

Exploiting Remark 1-8, the net force wrench on the right hand side of **Eq. 1-54** can be expressed (transformed) in terms of the frame $\{B_i\}$ as follows.

$$^{B_i}\bar{\boldsymbol{f}}^* = {}^{B_i}\boldsymbol{U}_{A_i}\, {}^{A_i}\bar{\boldsymbol{f}}_i^* = {}^{B_i}\boldsymbol{U}_{A_i} \begin{bmatrix} {}^{A_i}\boldsymbol{R}_I & \boldsymbol{0}_{3\times 3} \\ \boldsymbol{0}_{3\times 3} & {}^{A_i}\boldsymbol{R}_I \end{bmatrix} \begin{bmatrix} f_i^* \\ \boldsymbol{m}_i^* \end{bmatrix} \qquad\qquad \textbf{Eq. 1-55}$$

In similar manner, the velocity wrench can be represented in terms of the frame $\{B_i\}$ as

$$\bar{v}_i = \begin{bmatrix} v_i \\ w_i \end{bmatrix} = \begin{bmatrix} {}^{I}R_{A_i} & 0_{3\times3} \\ 0_{3\times3} & {}^{I}R_{A_i} \end{bmatrix} {}^{B_i}U_{A_i}^{T}\ {}^{B_i}\bar{v}_i \qquad\qquad \textbf{Eq. 1-56}$$

Differentiating **Eq. 1-56** results in

$$\dot{\bar{v}}_i = \begin{bmatrix} \dot{v}_i \\ \dot{w}_i \end{bmatrix} = \begin{bmatrix} (w_i\times)\ {}^{I}R_{A_i} & 0_{3\times3} \\ 0_{3\times3} & (w_i\times)\ {}^{I}R_{A_i} \end{bmatrix} {}^{B_i}U_{A_i}^{T}\ {}^{B_i}\bar{v}_i + \begin{bmatrix} {}^{I}R_{A_i} & 0_{3\times3} \\ 0_{3\times3} & {}^{I}R_{A_i} \end{bmatrix} {}^{B_i}U_{A_i}^{T}\ \frac{d}{dt}({}^{B_i}\bar{v}_i) \qquad \textbf{Eq. 1-57}$$

Substituting **Eq. 1-55** and **Eq. 1-57** into **Eq. 1-54** results in

$$M_{B_i}\ {}^{B_i}\dot{\bar{v}}_i + C_{B_i}({}^{B_i}w_i)\ {}^{B_i}\bar{v}_i + g_{B_i} = {}^{B_i}\bar{f}^* \qquad\qquad \textbf{Eq. 1-58}$$

with

$$M_{B_i} = \begin{bmatrix} m_i I_3 & -m_i({}^{B_i}r_{B_iA_i}\times) \\ m_i({}^{B_i}r_{B_iA_i}\times) & I_{B_i} - m_i({}^{B_i}r_{B_iA_i})^2 \end{bmatrix} \qquad\qquad \textbf{Eq. 1-59}$$

where I_{B_i} represents the configuration-free inertia tensor expressed in frame $\{B_i\}$

$$C_{B_i}({}^{B_i}w_i) = \begin{bmatrix} c_{11} & c_{12} \\ c_{21} & c_{22} \end{bmatrix} \qquad\qquad \textbf{Eq. 1-60}$$

with

$$c_{11} = m_i({}^{B_i}w_i\times),\ c_{12} = -m_i({}^{B_i}w_i\times)({}^{B_i}r_{B_iA_i}\times),\ c_{21} = m_i({}^{B_i}r_{B_iA_i}\times)({}^{B_i}w_i\times)$$

$$c_{22} = ({}^{B_i}w_i\times)I_{B_i} + I_{B_i}({}^{B_i}w_i\times) - m_i({}^{B_i}r_{B_iA_i}\times)({}^{B_i}w_i\times)({}^{B_i}r_{B_iA_i}\times)$$

$$g_{B_i} = \begin{bmatrix} m_i\ {}^{B_i}R_I g \\ m_i({}^{B_i}r_{B_iA_i}\times)\ {}^{B_i}R_I g \end{bmatrix} \qquad\qquad \textbf{Eq. 1-61}$$

   (ii) Dynamics of revolute joint subsystem

There are two types of drive transmission systems for robotic joint systems. The first is the direct drive joints, in which the inertia of the motor is included in the corresponding links [Zhu10, Spo89], such that the dynamics of the joint is neglected. The second type of the system deals with a high

gear transmission assuming that the inertial forces/torques act along the joint axis [Zhu10]. In the latter case, the dynamic equation of the joint (i) can be described as [Zhu10]

$$I_{J_i}\ddot{\theta}_i + \mathcal{k}_{ci}\,sign(\dot{\theta}_i) + \mathcal{k}_{vi}\dot{\theta}_i + \mathcal{k}_{si}\,sign(\dot{\theta}_i)\exp\left(-\left(\dot{\theta}_i/\eta_{si}\right)\right) + \mathcal{k}_{oi} = \tau_i^* \; (i$$
$$= 1,2,\dots,n_j)$$

Eq. 1-62

where I_{J_i} represents the equivalent inertia of the joint (i), $\ddot{\theta}_i$ denote the ith joint acceleration, τ_i^* represents the net torque applied to the joint (i), and n_j denotes the number of joints. The net torque of the joint (i) can be described as

$$\tau_i^* = \tau_{ci} - \mathbf{z}^T \, {}^{B_i}\bar{\mathbf{f}} \;\; (i = 1,2,\dots,n_j)$$

Eq. 1-63

where τ_{ci} is the input control torque of the joint (i) and the second term represents the output torque of the joint (i) towards the link (i).

1.2.2.2 Dynamics of the biped robot

Since the target biped is of a planar motion, simplifications appear in the dynamic equation of link (i) derived in **Eq. 1-58** to **Eq. 1-61** via the following:

(i)   Since the center of mass of link (i) is located on the $x-axis$ of frame $\{B_i\}$ with distance d_i from its its origin, ${}^{B_i}\mathbf{r}_{B_iA_i} = [d_i, 0, 0]^T$.

(ii)   Since there is orientation in z-axis only, ${}^{B_i}\mathbf{w} = [0, 0, w_{z_i}]^T$.

(iii) $I_{B_i} = diag(0, 0, I_{c_i})$.

(iv)   Removal of the third to the fifth rows/columns of $\mathbf{M}_{B_i}$ and $\mathbf{C}_{B_i}$.

Thus, the dynamics of planar biped robot can be expresses as in **Eq. 1-58** with the following dynamic coefficient matrices

$$\mathbf{M}_{B_i} = \begin{bmatrix} m_i & 0 & 0 \\ 0 & m_i & m_id_i \\ 0 & m_id_i & I_{ci} + m_id_i^2 \end{bmatrix}$$

Eq. 1-64

$$\mathbf{C}_{B_i} = \begin{bmatrix} 0 & -m_i & -m_id_i \\ m_i & 0 & 0 \\ m_id_i & m_id_i & 0 \end{bmatrix} w_{z_i} \text{ with } w_{z_i} = \dot{q}_i$$

Eq. 1-65

$$g_{B_i} = \begin{bmatrix} m_i \sin(q_i)\, g \\ m_i \cos(q_i)\, g \\ m_i\, d_i \cos(q_i)\, g \end{bmatrix}$$

Eq. 1-66

1.2.2.2.1 The SSP

As mentioned earlier, during this walking phase, the biped mechanism is an open chain mechanism with stance foot as fixed link; it should be in full contact with the ground. Therefore, the seven link-biped reduces to 6-link biped during its dynamic analysis. Three important points should be considered carefully when dealing with **Eq. 1-56** that are:

(i)   Determination of velocity wrench.

Solution of the dynamic **Eq. 1-56** needs finding the velocity wrench which plays an important role in the adaptive control problem; it can be found as follows. See **Fig. 1-5** for clear description of local frames.
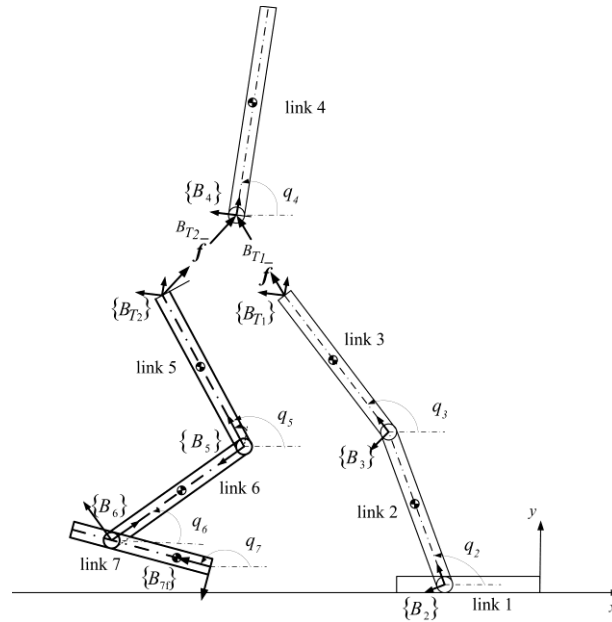
Fig. 1-5: Biped robot during the SSP with description of assumed local frames

Link (1) (stance foot link): It is assumed fixed link with negligible dynamics.

Link (2) (stance shank link):

$$x_{B_2} = -0.2 \; , \; \dot{x}_{B_2} = 0$$

Eq. 1-67

$$y_{B_2} = 0 \ , \ \dot{y}_{B_2} = 0 \tag{Eq. 1-68}$$

$$^{B_2}\overline{v} = \begin{bmatrix} 0 \\ 0 \\ \dot{q}_2 \end{bmatrix} \tag{Eq. 1-69}$$

Link (3) (stance thigh link):

$$x_{B_3} = -0.2 + l_2\cos(q_2) \ , \ \dot{x}_{B_3} = -l_2\sin(q_2)\dot{q}_2 \tag{Eq. 1-70}$$

$$y_{B_3} = l_2\sin(q_2) \ , \ \dot{y}_{B_3} = l_2\cos(q_2)\dot{q}_2 \tag{Eq. 1-71}$$

$$^{B_3}\overline{v} = \begin{bmatrix} \begin{bmatrix} \cos(q_3) & \sin(q_3) \\ -\sin(q_3) & \cos(q_3) \end{bmatrix} \begin{bmatrix} \dot{x}_{B_3} \\ \dot{y}_{B_3} \end{bmatrix} \\ \dot{q}_3 \end{bmatrix} = \begin{bmatrix} -l_2 \dot{q}_2 \sin(q_2 - q_3) \\ l_2 \dot{q}_2 \cos(q_2 - q_3) \\ \dot{q}_3 \end{bmatrix} \tag{Eq. 1-72}$$

Link (4) (Trunk):

$$x_{B_4} = -0.2 + l_2 \cos(q_2) + l_3 \cos(q_3) \ , \ \dot{x}_{B_4} = -l_2 \sin(q_2) \dot{q}_2 - l_3 \sin(q_3) \dot{q}_3 \tag{Eq. 1-73}$$

$$y_{B_4} = l_2 \sin(q_2) + l_3 \sin(q_3) \ , \ \dot{y}_{B_4} = l_2 \cos(q_2) \dot{q}_2 + l_3 \cos(q_3) \dot{q}_3 \tag{Eq. 1-74}$$

$$^{B_4}\overline{v} = \begin{bmatrix} \begin{bmatrix} \cos(q_4) & \sin(q_4) \\ -\sin(q_4) & \cos(q_4) \end{bmatrix} \begin{bmatrix} \dot{x}_{B_4} \\ \dot{y}_{B_4} \end{bmatrix} \\ \dot{q}_4 \end{bmatrix}$$

$$= \begin{bmatrix} -l_2 \dot{q}_2 \sin(q_2 - q_4) - l_3 \dot{q}_3 \sin(q_3 - q_4) \\ l_2 \dot{q}_2 \cos(q_2 - q_4) + l_3 \dot{q}_3 \cos(q_3 - q_4) \\ \dot{q}_4 \end{bmatrix} \tag{Eq. 1-75}$$

Link (5)(swing thigh link):

$$x_{B_5} = -0.2 + l_2 \cos(q_2) + l_3 \cos(q_3) - l_5 \cos(q_5), \ \dot{x}_{B_5} = -l_2 \sin(q_2) \dot{q}_2 - l_3 \sin(q_3) \dot{q}_3 + l_5\sin(q_5)\dot{q}_5 \tag{Eq. 1-76}$$

$$y_{B_5} = l_2 \sin(q_2) + l_3 \sin(q_3) - l_5 \sin(q_5)$$

$$\dot{y}_{B_5} = l_2 \cos(q_2) \dot{q}_2 + l_3 \cos(q_3) \dot{q}_3 - l_5\cos(q_5)\dot{q}_5 \tag{Eq. 1-77}$$

$$
{}^{B_5}\overline{v} = \begin{bmatrix} \begin{bmatrix} \cos(q_5) & \sin(q_5) \\ -\sin(q_5) & \cos(q_5) \end{bmatrix} \begin{bmatrix} \dot{x}_{B_5} \\ \dot{y}_{B_5} \end{bmatrix} \\ \dot{q}_5 \end{bmatrix}
$$

$$
= \begin{bmatrix} -l_2\,\dot{q}_2\sin(q_2 - q_5) - l_3\,\dot{q}_3\sin(q_3 - q_5) \\ l_2\,\dot{q}_2\cos(q_2 - q_5) - l_5\dot{q}_5 + l_3\,\dot{q}_3\cos(q_3 - q_5) \\ \dot{q}_5 \end{bmatrix}
$$

Eq. 1-78

Link (6) (swing shank link):

$$
x_{B_6} = -0.2 + l_2\cos(q_2) + l_3\cos(q_3) - l_5\cos(q_5) - l_6\cos(q_6)
$$

$$
\dot{x}_{B_6} = -l_2\sin(q_2)\,\dot{q}_2 - l_3\sin(q_3)\,\dot{q}_3 + l_5\sin(q_5)\,\dot{q}_5 + l_6\sin(q_6)\,\dot{q}_6
$$

Eq. 1-79

$$
y_{B_6} = l_2\sin(q_2) + l_3\sin(q_3) - l_5\sin(q_5) - l_6\sin(q_6)
$$

$$
\dot{y}_{B_6} = l_2\cos(q_2)\,\dot{q}_2 + l_3\cos(q_3)\,\dot{q}_3 - l_5\cos(q_5)\,\dot{q}_5 - l_6\cos(q_6)\dot{q}_6
$$

Eq. 1-80

$$
{}^{B_6}\overline{v} = \begin{bmatrix} \begin{bmatrix} \cos(q_6) & \sin(q_6) \\ -\sin(q_6) & \cos(q_6) \end{bmatrix} \begin{bmatrix} \dot{x}_{B_6} \\ \dot{y}_{B_6} \end{bmatrix} \\ \dot{q}_6 \end{bmatrix}
$$

$$
= \begin{bmatrix} l_5\,\dot{q}_5\sin(q_5 - q_6) - l_2\,\dot{q}_2\sin(q_2 - q_6) - l_3\,\dot{q}_3\sin(q_3 - q_6) \\ l_2\,\dot{q}_2\cos(q_2 - q_6) - l_6\dot{q}_6 + l_3\,\dot{q}_3\cos(q_3 - q_6) - l_5\,\dot{q}_5\cos(q_3 - q_6) \\ \dot{q}_6 \end{bmatrix}
$$

Eq. 1-81

Link (7) (swing foot link):

$$
x_{B_7} = -0.2 + l_2\cos(q_2) + l_3\cos(q_3) - l_5\cos(q_5) - l_6\cos(q_6) - l_{7a}\cos(q_7)
$$

$$
\dot{x}_{B_7} = -l_2\sin(q_2)\,\dot{q}_2 - l_3\sin(q_3)\,\dot{q}_3 + l_5\sin(q_5)\,\dot{q}_5 + l_6\sin(q_6)\,\dot{q}_6 \\ + l_{7a}\sin(q_7)\,\dot{q}_7
$$

Eq. 1-82

$$
y_{B_7} = l_2\sin(q_2) + l_3\sin(q_3) - l_5\sin(q_5) - l_6\sin(q_6) - l_{7a}\sin(q_7)
$$

$$
\dot{y}_{B_7} = l_2\cos(q_2)\,\dot{q}_2 + l_3\cos(q_3)\,\dot{q}_3 - l_5\cos(q_5)\,\dot{q}_5 - l_6\cos(q_6)\,\dot{q}_6 \\ - l_{7a}\cos(q_7)\,\dot{q}_7
$$

Eq. 1-83

$$B_6\overline{v} = \begin{bmatrix} \begin{bmatrix} \cos(q_6) & \sin(q_6) \\ -\sin(q_6) & \cos(q_6) \end{bmatrix} \begin{bmatrix} \dot{x}_{B_7} \\ \dot{y}_{B_7} \end{bmatrix} \\ \dot{q}_7 \end{bmatrix}$$

$$= \begin{bmatrix} l_5\,\dot{q}_5\sin(q_5-q_7) + l_6\,\dot{q}_6\sin(q_6-q_7)-l_2\,\dot{q}_2\sin(q_2-q_6)- l_3\,\dot{q}_3\sin(q_3-q_6) \\ l_2\,\dot{q}_2\cos(q_2-q_7) - l_{7a}\dot{q}_7 + l_3\,\dot{q}_3\cos(q_3-q_7) - l_5\,\dot{q}_5\cos(q_3-q_7) - l_6\,\dot{q}_6\cos(q_6-q_7) \\ \dot{q}_7 \end{bmatrix}$$
Eq. 1-84

   (ii)   Resultant force wrench

To understand the force wrench distribution at the torso/leg interaction, see **Fig. 1-5**. Thus, the following relations can be expressed for each link starting from the trunk.

Link (4) (trunk):

$$^{B_4}\overline{f}^* = {}^{B_{T1}}\overline{f} + {}^{B_{T2}}\overline{f}$$
Eq. 1-85

with notations shown in **Fig. 1-5**.

Link (5)(swing thigh):

$$^{B_5}\overline{f}^* = {}^{B_5}\overline{f} - {}^{B_5}U_{B_4}{}^{B_{T2}}\overline{f}$$
Eq. 1-86

with

$$^{B_5}U_{B_4} = {}^{B_5}U_T\,{}^{B_4}U_T{}^{-1} = \begin{bmatrix} {}^{B_5}R_T & \begin{bmatrix}0\\0\end{bmatrix} \\ -l_5\cos(q_5) & -l_5\sin(q_5) & 1 \end{bmatrix}\begin{bmatrix} {}^{B_5}R_T & \begin{bmatrix}0\\0\end{bmatrix} \\ 0 & 0 & 1 \end{bmatrix}$$

$$= \begin{bmatrix} \cos(q_5) & \sin(q_5) & 0 \\ -\sin(q_5) & \cos(q_5) & 0 \\ -l_5\cos(q_5) & -l_5\sin(q_5) & 1 \end{bmatrix}\begin{bmatrix} \cos(q_4) & -\sin(q_4) & 0 \\ \sin(q_4) & \cos(q_4) & 0 \\ 0 & 0 & 1 \end{bmatrix}$$

$$= \begin{bmatrix} \cos(q_5-q_4) & \sin(q_5-q_4) & 0 \\ -\sin(q_5-q_4) & \cos(q_5-q_4) & 0 \\ -l_5\cos(q_5-q_4) & -l_5\sin(q_5-q_4) & 1 \end{bmatrix}$$
Eq. 1-87

Link (6) (swing shank):

$$^{B_6}\overline{f}^* = {}^{B_6}\overline{f} - {}^{B_6}U_{B_5}{}^{B_5}\overline{f}$$
Eq. 1-88

with

$$
{}^{B_6}\boldsymbol{U}_{B_5} = \begin{bmatrix} & {}^{B_6}\boldsymbol{R}_{B_5} & \begin{bmatrix} 0 \\ 0 \end{bmatrix} \\ l_6 \sin(q_5 - q_6) & l_6 \cos(q_5 - q_6) & 1 \end{bmatrix}
$$

$$
= \begin{bmatrix} \cos(q_5 - q_6) & -\sin(q_5 - q_6) & 0 \\ \sin(q_5 - q_6) & \cos(q_5 - q_6) & 0 \\ l_6 \sin(q_5 - q_6) & l_6 \cos(q_5 - q_6) & 1 \end{bmatrix}
$$

Eq. 1-89

Link (7) (swing foot):

$$
{}^{B_7}\overline{\boldsymbol{f}}^* = {}^{B_7}\overline{\boldsymbol{f}} - {}^{B_7}\boldsymbol{U}_{B_6} \, {}^{B_6}\overline{\boldsymbol{f}}
$$

Eq. 1-90

with

$$
{}^{B_7}\boldsymbol{U}_{B_6} = \begin{bmatrix} \cos(q_6 - q_7) & -\sin(q_6 - q_7) & 0 \\ \sin(q_6 - q_7) & \cos(q_6 - q_7) & 0 \\ l_6 \sin(q_6 - q_7) & l_6 \cos(q_6 - q_7) & 1 \end{bmatrix}
$$

Eq. 1-91

Link (3) (stance thigh):

$$
{}^{B_3}\overline{\boldsymbol{f}}^* = {}^{B_3}\overline{\boldsymbol{f}} - {}^{B_3}\boldsymbol{U}_{B_4} \, {}^{B_{T_1}}\overline{\boldsymbol{f}}
$$

Eq. 1-92

with

$$
{}^{B_3}\boldsymbol{U}_{B_4} = \begin{bmatrix} \cos(q_3 - q_4) & \sin(q_3 - q_4) & 0 \\ -\sin(q_3 - q_4) & \cos(q_3 - q_4) & 0 \\ -l_3 \sin(q_3 - q_4) & l_3 \cos(q_3 - q_4) & 1 \end{bmatrix}
$$

Eq. 1-93

Link (2)(stance shank):

$$
{}^{B_2}\overline{\boldsymbol{f}}^* = {}^{B_2}\overline{\boldsymbol{f}} - {}^{B_2}\boldsymbol{U}_{B_3} \, {}^{B_3}\overline{\boldsymbol{f}}
$$

Eq. 1-94

with

$$
{}^{B_2}\boldsymbol{U}_{B_3} = \begin{bmatrix} \cos(q_3 - q_2) & -\sin(q_3 - q_2) & 0 \\ \sin(q_3 - q_2) & \cos(q_3 - q_2) & 0 \\ l_2 \sin(q_3 - q_2) & l_2 \cos(q_3 - q_2) & 1 \end{bmatrix}
$$

Eq. 1-95

We note that we have 6 equations for six links(**Eq. 1-85**, **Eq. 1-86**, **Eq. 1-88**, **Eq. 1-90**, **Eq. 1-92**, **Eq. 1-94**), with 7 unknowns ($^{B_{T1}}\bar{f}$, $^{B_{T2}}\bar{f}$, $^{B_5}\bar{f}$, $^{B_6}\bar{f}$, $^{B_7}\bar{f}$, $^{B_3}\bar{f}$, $^{B_2}\bar{f}$). Because the swing foot does not have force wrench at the frame $\{B_7\}$, so $^{B_7}\bar{f} = \mathbf{0}$. Thus, $^{B_6}\bar{f}$ can recursively be calculated from **Eq. 1-90** and so on.

(iii)   Actuating torques

To simplify the analysis, let us assume temporarily that the target biped has direct drive joint systems (the dynamics of the joint could be included with the corresponding links [Zhu10, Spo89]) the left hand side of **Eq. 1-63** is equal to zero. Consequently, the actuating torques can be calculated from the coupling effect of the neighbored link according to **Eq. 1-63**.

$$\text{Left shank, } \tau_{c1} = \mathbf{z}^T {}^{B_2}\bar{f} \qquad\qquad \textbf{Eq. 1-96}$$

$$\text{Left knee, } \tau_{c2} = \mathbf{z}^T {}^{B_3}\bar{f} \qquad\qquad \textbf{Eq. 1-97}$$

$$\text{Left thigh/torso interaction, } \tau_{c3} = \mathbf{z}^T {}^{B_{T1}}\bar{f} \qquad\qquad \textbf{Eq. 1-98}$$

$$\text{Right thigh/torso interaction, } \tau_{c4} = \mathbf{z}^T {}^{B_{T2}}\bar{f} \qquad\qquad \textbf{Eq. 1-99}$$

$$\text{Right knee, } \tau_{c5} = \mathbf{z}^T {}^{B_5}\bar{f} \qquad\qquad \textbf{Eq. 1-100}$$

$$\text{Right shank, } \tau_{c6} = \mathbf{z}^T {}^{B_6}\bar{f} \qquad\qquad \textbf{Eq. 1-101}$$

1.2.2.2.2   The DSP1

As mentioned earlier, the biped in this walking sub-phase, DSP1, has six actuators with 4 DOFs; therefore, two redundant actuators compromise the over-actuation problem. In the following, the details of velocity and force wrenches as well as determining the redundant actuating torques are investigated.

- Velocity wrench. It has exactly the same relations described in previous subsection, **Eq. 1-67** to **Eq. 1-84** with replacing the word (swing) by (front), the word (stance) to (rear), and l_{7a} by $(l_7 - l_{7a})$ for the last link.
- Force wrench. It has also the same force wrenches showed in **Eq. 1-85** to **Eq. 1-95**.
- Actuating torques. We have three significant problems resulting from the variable configurations of the biped which include: (a) redundancy of the actuators, (b) the passive

joint on the front foot (see **Fig. 1-6**) which enforces the torque to be $\tau_{c_f} = 0$, and (c) the discontinuity of the actuating torques. Four solutions are considered below with focus on solutions 3 and 4 which can be ranked best among the rest.
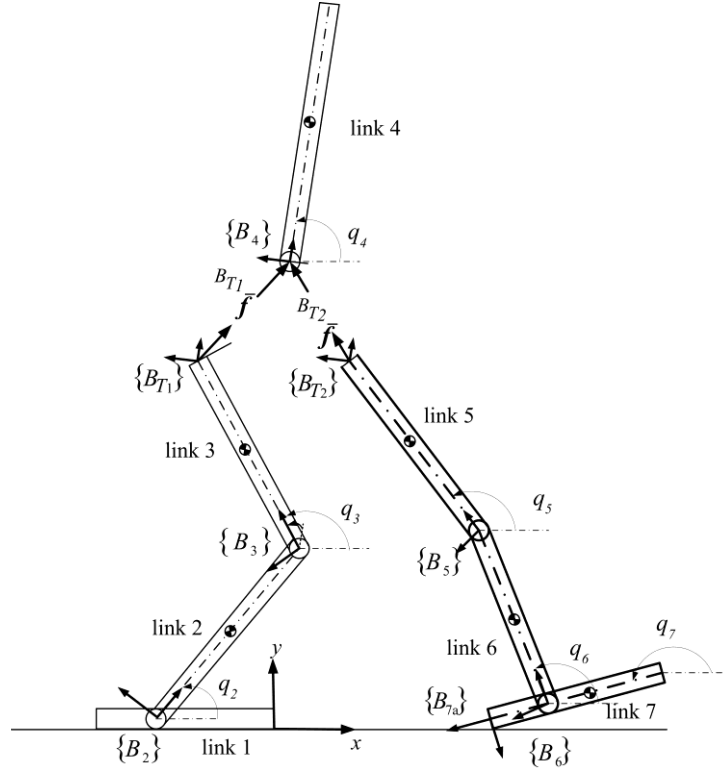
Fig. 1-6: Biped robot during the DSP1

(i) Procedure 1-releasing and optimizing the internal forces

This strategy assumes that the biped resembles two cooperating manipulators (two legs) holding one object (the trunk of the biped robot). Thus, the two interaction force wrenches, ${}^{B_{T_1}}\bar{f}$ and ${}^{B_{T_2}}\bar{f}$ can be expressed as [Zhu10]

$$
{}^{B_{T_1}}\bar{f} = \sigma\, {}^{B_4}\bar{f}^* + \eta
$$

<div align="right">Eq. 1-102</div>

$$
{}^{B_{T_2}}\bar{f} = (1 - \sigma)\, {}^{B_4}\bar{f}^* - \eta
$$

<div align="right">Eq. 1-103</div>

with $\eta \in \mathbb{R}^3$ denotes the internal force wrench and σ is a scalar value bounded by 0 and 1 ($0 \leq \sigma \leq 1$).

Then, describing the actuating torques in terms of the design variables (η).

$$\tau = B_1\eta + b_1$$

<div align="right">Eq. 1-104</div>

with the constraint of passive joint

$$\tau_{c_f} = 0 = a_1{}^T\eta + a_2$$

<div align="right">Eq. 1-105</div>

By defining the objective function

$$\sigma = \frac{1}{2}\,\tau^T W\tau$$

<div align="right">Eq. 1-106</div>

where $W \in \mathbb{R}^{6\times6}$ is a symmetric weighting matrix; it is assumed as an identity matrix in our solution.

Substituting **Eq. 1-104** into **Eq. 1-106** and incorporating the constraint of **Eq. 4-105** to get

$$\sigma = \frac{1}{2}(B_1\eta + b_1)^T W(B_1\eta + b_1) + \mathcal{G}(a_1{}^T\eta + a_2)$$

<div align="right">Eq. 1-107</div>

Differentiating **Eq. 1-107** with respect to η and setting it to zero

$$\eta = -(B_1{}^T W B_1)^{-1}B_1{}^T W b_1 - (B_1{}^T W B_1)^{-1}a_1\,\mathcal{G}$$

<div align="right">Eq. 1-108</div>

Substituting **Eq. 1-108** into **Eq. 1-105** to yield

$$\mathcal{G} = \frac{a_2 - a_1{}^T(B_1{}^T W B_1)^{-1}B_1{}^T W b_1}{a_1{}^T(B_1{}^T W B_1)^{-1}a_1}$$

<div align="right">Eq. 1-109</div>

Substituting **Eq. 1-109** into **Eq. 1-108** to get the internal force wrench

$$\eta = -(B_1{}^T W B_1)^{-1}B_1{}^T W b_1$$
$$- (B_1{}^T W B_1)^{-1}a_1\left(\frac{a_2 - a_1{}^T(B_1{}^T W B_1)^{-1}B_1{}^T W b_1}{a_1{}^T(B_1{}^T W B_1)^{-1}a_1}\right)$$

<div align="right">Eq. 1-110</div>

Thus, the force wrench at the torso can be determined from **Eq. 1-85**, and sequentially finding the rest force wrenches and the required torques via the following **Eq. 1-86**, **Eq. 1-88**, **Eq. 1-90**,**Eq. 1-92**,**Eq. 1-94**, **Eq. 1-96** to **Eq. 1-101**. The disadvantages of this procedure is that σ is a free parameter; it has not been considered as design variable, and there is also no guarantee to satisfy continuous dynamic response related to actuating torques.

(ii) Procedure 2- direct optimization of the torso/leg force wrench

Instead of releasing internal force wrench, the actuating torques can directly be expressed in terms of $^{B_{T1}}\bar{f}$ or $^{B_{T2}}\bar{f}$. Thus, we can get the same equations above but in terms of $^{B_{T1}}\bar{f}$ as follows.

$$^{B_{T1}}\bar{f} = -(B_1{}^T wB_1)^{-1}B_1{}^T wb_1$$
$$- (B_1{}^T wB_1)^{-1}a_1\left(\frac{a_2 - a_1{}^T(B_1{}^T wB_1)^{-1}B_1{}^T wb_1}{a_1{}^T(B_1{}^T wB_1)^{-1}a_1}\right) \qquad \textbf{Eq.1-111}$$

and completing the same steps as of the procedure 1. However, the discontinuity problem has not been resolved in the above two procedures.

(iii) Procedure 3- tracking desired ground reaction forces.

Considering Assumption 1-4 and assuming the desired reaction force, see **Eq. 1-41**, as a constraint to yield

$$^{B_7}\bar{f} = \begin{bmatrix} \lambda \\ \tau_{c_f} \end{bmatrix} = \breve{B}\ ^{B_{T1}}\bar{f} + \breve{b} \qquad \textbf{Eq.1-112}$$

with $\breve{B} \in \mathbb{R}^{3\times3}$ and $\breve{b} \in \mathbb{R}^3$.

The left hand side of **Eq.1-112** is known from the desired walking trajectories, so the problems of over-actuating and discontinuity are solved using the last equation without need of optimization.

Remark 1-11. If the number of constraints is equal to the design variables, no optimization of the system is necessary because the solution of equality constraints are the only candidates for the optimum design [Aro12].

(iv) Procedure 4- tracking desired ground reaction forces with optimization

In this procedure, we will come back to procedure 1 representing the trunk/leg interaction force wrench in terms of the internal force wrench and α parameter. Thus, constraint **Eq.1-112** can be expressed as follows

$$^{B_7}\bar{f} = \begin{bmatrix} \lambda \\ \tau_{c_f} \end{bmatrix} = B_2\eta + b_2\sigma + b_3 \qquad \textbf{Eq. 1-113}$$

with $B_2 \in \mathbb{R}^{3\times3}$, $b_2 \in \mathbb{R}^3$ and $b_3 \in \mathbb{R}^3$. Re-arranging **Eq. 1-113** and using the pseudo-inverse definition

$$\begin{bmatrix} \boldsymbol{\eta} \\ \bar{\sigma} \end{bmatrix} = [\boldsymbol{B}_2 \quad \boldsymbol{b}_2]^{\neq} \left({}^{B_7}\bar{\boldsymbol{f}} - \boldsymbol{b}_3 \right) \tag{Eq.1-114}$$

where $\bar{\sigma}$ denotes the candidate optimal solution. Because of the bounded limits of σ, the following procedure is proposed:

$$\text{If } 0 \leq \bar{\sigma} \leq 1, \text{ then } \sigma = \bar{\sigma}.$$

$$\text{If } \bar{\sigma} \geq 1, \text{ then } \sigma = 1. \tag{Eq.1-115}$$

$$\text{If } \bar{\sigma} \leq 0, \text{ then } \sigma = 0.$$

After finding the internal force wrench and α parameter, it is easy to find the actuating torques in a similar way described previously (see procedure 1).

1.2.2.2.3 The DSP2

In this walking sub-phase, the biped robot has two redundant actuators with a slightly different configuration of that of DSP1 (see **Fig. 1-7**). Here, the front foot is flat on the ground with negligible dynamics while the rear foot rotates about its front tip. In similar manner to DSP1, the velocity wrench of each link can be determined as made in Subsection 1.2.2.2.1, whereas, the force wrench can be calculated successfully using procedure 1 described in the previous subsection.

- Velocity wrench. It is exactly determined in the same manner used in the SSP and DSP1; therefore, we will list only the final results of each link without details.

Link (1) (rear foot):
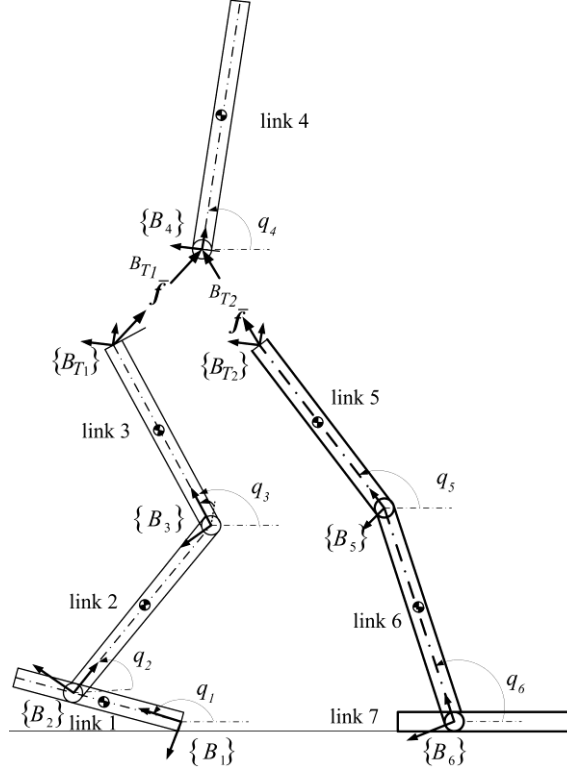
$$^{B_1}\bar{\boldsymbol{v}} = \begin{bmatrix} 0 \\ 0 \\ \dot{q}_1 \end{bmatrix} \tag{Eq.1-116}$$

Link (2) (rear shank):

$$^{B_2}\bar{\boldsymbol{v}} = \begin{bmatrix} -l_{1a} \, \dot{q}_1 \sin(q_1 - q_2) \\ l_{1a} \, \dot{q}_1 \cos(q_1 - q_2) \\ \dot{q}_2 \end{bmatrix} \tag{Eq.1-117}$$

Link (3) (rear thigh):

$$
^{B_3}\overline{\boldsymbol{v}} = \begin{bmatrix} -l_1\dot{q}_2\sin(q_2 - q_3) - l_{1a}\,\dot{q}_1\sin(q_1 - q_3) \\ l_1\dot{q}_2\cos(q_2 - q_3) + l_{1a}\,\dot{q}_1\cos(q_1 - q_3) \\ \dot{q}_3 \end{bmatrix} \qquad \textbf{Eq.1-118}
$$

Fig. 1-7: Biped robot during the DSP2

Link (4) (trunk):

$$
^{B_4}\overline{\boldsymbol{v}} = \begin{bmatrix} -l_1\dot{q}_2\sin(q_2 - q_4) - l_2\dot{q}_3\sin(q_3 - q_4) - l_{1a}\,\dot{q}_1\sin(q_1 - q_4) \\ l_1\dot{q}_2\cos(q_2 - q_4) + l_2\dot{q}_3\cos(q_3 - q_4) + l_{1a}\,\dot{q}_1\cos(q_1 - q_4) \\ \dot{q}_4 \end{bmatrix} \qquad \textbf{Eq.1-119}
$$

Link (5) (front thigh):

$$
^{B_5}\overline{\boldsymbol{v}}
$$
$$
= \begin{bmatrix} -l_1\dot{q}_2\sin(q_2 - q_5) - l_2\dot{q}_3\sin(q_3 - q_5) - l_{1a}\,\dot{q}_1\sin(q_1 - q_5) \\ l_1\dot{q}_2\cos(q_2 - q_5) - l_4\dot{q}_5 + l_2\dot{q}_3\cos(q_3 - q_5) + l_{1a}\,\dot{q}_1\cos(q_1 - q_5) \\ \dot{q}_5 \end{bmatrix} \qquad \textbf{Eq.1-120}
$$

Link (6) (front shank):

$$
{}^{B_6}\overline{\boldsymbol{v}} = \begin{bmatrix} {}^{B_6}v_{\mathrm{x}} \\ {}^{B_6}v_{\mathrm{y}} \\ {}^{B_6}w_{\mathrm{z}} \end{bmatrix}
$$

with

$$
\begin{aligned}
{}^{B_6}v_{\mathrm{x}} &= -l_4\dot{q}_5\sin(q_5 - q_6) - l_2\dot{q}_3\sin(q_3 - q_6) - l_1\dot{q}_2\sin(q_2 - q_6) \\
&\quad - l_{1a}\,\dot{q}_1\sin(q_1 - q_6) \\
{}^{B_6}v_{\mathrm{y}} &= l_1\dot{q}_2\cos(q_2 - q_6) - l_5\dot{q}_6 + l_2\dot{q}_3\cos(q_3 - q_6) - l_4\dot{q}_5\cos(q_5 - q_6) \\
&\quad + l_{1a}\,\dot{q}_1\cos(q_1 - q_6)
\end{aligned}
$$
Eq.1-121

$$
{}^{B_6}w_{\mathrm{z}} = \dot{q}_6
$$

- Force wrench. The same relationships of **Eq. 1-85** to **Eq. 1-95** hold .
- Actuating torques. Procedure 3 or 4 can be used to solve the problem of over-actuation and discontinuity during this walking sub-phase. After finding the internal force wrench and α parameter as described in **Eq. 1-113** to **Eq.1-115**, the actuating torques can be determined by **Eq. 1-96** to **Eq. 1-101.**

2   Conclusions and future work

In this work, we have modeled two selected walking patterns of biped robot using Lagrangian and virtual decomposition-based N-E formulation. The problem of discontinuity is solved using linear transition ground reaction forces without impact-contact event. Lagrangian formulation, unless simplified, could require more computational complexity than that of virtual decomposition-based N-E formulation.

3   References

[Alb12] Alba, A. G.; Zielinska, T. *Postural equilibrium criteria concerning feet properties for biped robot.* Journal of Automation, mobile robotics and Intelligent Systems: 6 (1), 22-27, 2012.

[Aro12] Arora, J. S. *Introduction to optimum design.* USA: Elsevier, 2012.

[Fu87] Fu, K. S.; Gonzalez, R. C.; C. Lee, S. G. *Robotics: control, sensing, vision, and intelligence* USA: McGraw-Hill Book Company, 1987.

[Hay13/1] Al-Shuka, Hayder F. N; Corves, B. *On the walking pattern generators of biped robot.* Journal of Automation and Control, Vol.1, No. 2, pp.149-156 (March 2013) http://www.joace.org/uploadfile/2013/0506/20130506045849456.pdf.

[Hay13/2] Al-Shuka, Hayder F. N; Corves, B.; Zhu, Wen-Hong. *On the dynamic optimization of biped robot.* Lecture Notes on Software Engineering, Vol. 1, No. 3, pp. 237-243 (June 2013) https://pdfs.semanticscholar.org/856d/42547334681b2afe79067d52fc9b0103d8ee.pdf.

[Hay13/3] Al-Shuka, Hayder F. N; Corves, B.; Vanderborght, B.; Zhu, Wen-Hong. *Finite difference-based suboptimal trajectory planning of biped robot with continuous dynamic response.* International Journal of Modeling and Optimization, Vol.3, No. 4, pp.337-343 (August 2013) http://www.ijmo.org/papers/294-CS0019.pdf.

[Hay14/1] Al-Shuka, Hayder F. N; Corves, B.; Zhu, Wen-Hong; Vanderborght, B. *A Simple algorithm for generating stable biped walking patterns.* International Journal of Computer Applications, Vol. 101, No. 4, pp. 29-33 (Sep. 2014) https://pdfs.semanticscholar.org/57ec/9c1fdde5b50468c6ef5881ef33a97a55168d.pdf.

[Hay14/2] Al-Shuka, Hayder F. N; Corves, B.; Zhu, Wen-Hong. *Dynamic modeling of biped robot using Lagrangian and recursive Newton-Euler formulations.* International Journal of Computer Applications, Vol. 101, No. 3, pp. 1-8 (Sep. 2014) http://citeseerx.ist.psu.edu/viewdoc/download?doi=10.1.1.800.2667&rep=rep1&type=pdf.

[Hay14/3] Al-Shuka, Hayder F. N; Allmedinger, F; Corves, B.; Zhu, Wen-Hong. *Modeling, stability and walking pattern generators of biped robots: a review.* Robotica, Cambridge Press, Vol. 32, No. 6, pp. 907-934 (Sep. 2014) https://doi.org/10.1017/S0263574713001124.

[Hay14/4] Al-Shuka, Hayder F. N; Corves, B.; Zhu, Wen-Hong. *Function approximation technique-based adaptive virtual decomposition control for a serial-chain manipulator.* Robotica, Cambridge Press, Vol. 32, No. 3, pp. 375-399 (May 2014) https://doi.org/10.1017/S0263574713000775.

[Hay14] Al-Shuka, Hayder F. N. *Modeling, walking pattern generators and adaptive control of biped robot.* PhD Dissertation, RWTH Aachen University, Department of Mechanical Engineering, IGM, Germany (2014) http://publications.rwth-aachen.de/record/465562.

[Hay15] Al-Shuka, Hayder F. N; Corves, B.; Vanderborght, B.; Zhu, Wen-Hong. *Zero-moment point-based biped robot with different walking patterns.* International Journal of Intelligent Systems and Applications, Vol. 07, No. 1, pp. 31-41 (2015) https://www.researchgate.net/publication/267865541_Zero-Moment_Point-Based_Biped_Robot_with_Different_Walking_Patterns.

[Hay16] Al-Shuka, Hayder F. N; Corves, B.; Zhu, Wen-Hong; Vanderborght, B. *Multi-level control of zero moment point-based biped humanoid robots: a review.* Robotica, Cambridge Press, vol. 34, No. 11, pp. 2440-2466 (2016) https://doi.org/10.1017/S0263574715000107.

[Hay17/1] Al-Shuka, Hayder F. N. *Stress distribution and optimum design of polypropylene and laminated transtibial prosthetic sockets: FEM and experimental implementations.* Munich, GRIN Verlag (2017) https://www.grin.com/document/385910.

[Hay17/2] Al-Shuka, Hayder F. N. *An overview on balancing and stabilization control of biped robots.* Munich, GRIN Verlag (2017) https://www.grin.com/document/375226

[Hay18/1] Al-Shuka, Hayder F. N.; Song, R. *On low-level control strategies of lower extremity exoskeletons with power augmentation.* The 10th IEEE International Conference on Advanced Computational Intelligence, Xiamen, China, pp. 63-68 (2018) DOI**:**10.1109/ICACI.2018.8377581.

[Hay18/2] Al-Shuka, Hayder F. N.; Song, R. *On high-level control of power-augmentation lower extremity exoskeleton: human walking intention.* The 10th IEEE International Conference on

Advanced Computational Intelligence, Xiamen, China, pp. 169-174 (2018) DOI: 10.1109/ICACI.2018.8377601.

[Hay18/3] Al-Shuka, Hayder F. N. *On local approximation-based adaptive control with applications to robotic manipulators and biped robot.* International Journal of Dynamics and Control, Springer, Vol. 6, No. 1, pp. 393-353 (2018) https://doi.org/10.1007/s40435-016-0302-6.

[Hay 18/4] Al-Shuka, Hayder F. N. Design of walking patterns for zero-momentum point (ZMP)-based biped robots: a computational optimal control approach, Munich, GRIN Verlag (2018) https://www.grin.com/document/434367.

[Hay19] Al-Shuka, Hayder F. N.; Song, R. *Decentralized Adaptive Partitioned Approximation Control of Robotic Manipulators.* In: Arakelian V., Wenger P. (eds), ROMANSY 22 – Robot Design, Dynamics and Control. CISM International Centre for Mechanical Sciences (Courses and Lectures), vol 584. Springer, Cham (2019) https://doi.org/10.1007/978-3-319-78963-7_3.

[Hol80]   Hollerbach, J. M. *A recursive lagrangian formulation of manipulator dynamics and comparative study of dynamics formulation complexity*   IEEE. Trans. On Systems, Man, and cybernetics: SMC-10 (11), 730-736, 1980.

[Kha11]   Khalil, W. *Dynamic modeling of robots using recursive Newton-Euler formulations* . A. Cettoet al. (Eds.): Informatics in Control, Automation and Robotic, LNEE 89, pp. 3-20, Springer-Verlag Berlin Heidelberg, 2011.

[Lee83]   Lee, C. S. G.; Lee, B. H.; Nigam, R. *Development of the generalized d'Alembert equations of motions for mechanical manipulators.* Proc. Conf. Decision and Control, San Antonio, Tex., pp. 1205-1210 (1983).

[Mit97]   Mitobe, K.; Mori, N.; Nasu, Y.; Adachi, N. *Control of a biped walking robot during the double support phase* Autonomous Robots: 4(3), 287-296, 1997.

[Moh07]   Mohan, A.; Saha, S. K. *A recursive, numerically stable and efficient simulation algorithm for serial robots* Int. J. Multibody System Dynamics: 17(4), 291-319, 2007.

[Pen07]   Pennestri, E.; Valentini, P. P. *Coordinate reduction strategies in multibody dynamics: a review.* In Atti Conference on Multibody System Dynamics, 2007.

[Sam08] Radhi, S.; Al-Shuka, Hayder F. N. *Analysis of below knee prosthetic socket.* Journal of Engineering and Development, Vol. 12, No.2, pp. 127-136 (June 2008) https://www.iasj.net/iasj?func=fulltext&aId=10094.

[Sat10]Sato, T.; Sakaino, S.; Ohnishi, K. *Trajectory planning and control for biped robot with toe and heel joint.* IEEE International Workshop on Advanced Motion Control, Nagaoka, Japan, pp.129-136 (March 2010).

[Spo89]   Spong, Mark. W.; Vidyasagar, M. *Robot dynamics and control.* USA: John Wiley & Sons, 1989.

[Su90] Su, C.-Y.; Leung, T. P.; Zhou, Q.-J. *Adaptive control of robot manipulators under constrained motion.* Proceedings of the 29th Conference on Decision and Control, pp. 2650-2655 (1990).

[Tsa99]   Tsai, Lung-Wen. *Robot analysis: the mechanics of serial and parallel manipulators.* New York: John Wiley and Sonc Inc, 1999.

[Van08]   Vanderborght, B.; Ham, R. V.; Verrelst, B.; Damme, M. V.; Lefeber, D. *Overview of the Lucy project: Dynamic stabilization of a biped powered by pneumatic artificial muscles* Advanced Robotics: 22 (10), 1027-1051, 2008.

[Zhu10]   Zhu, W.-H *Virtual decomposition control: towards hyper degrees of freedom* Berlin, Germany: Springer–Verlag, 2010.